Biomedical Engineering Letters (2018) 8:157–165
https://doi.org/10.1007/s13534-018-0070-7

REVIEW ARTICLE

Development and clinical translation of photoacoustic mammography

Tsuyoshi Shiina[1] · Masakazu Toi[2] · Takayuki Yagi[3]

Received: 21 March 2018 / Revised: 21 April 2018 / Accepted: 23 April 2018 / Published online: 7 May 2018

Abstract
To practically apply photoacoustic (PA) imaging technology in medicine, we have developed prototypes of a photoacoustic mammography (PAM) device to acquire images for diagnosing breast cancer in the Kyoto University/Canon joint research project (CK project supported by MEXT, Japan). First, the basic ability of the PAM system to visualize the network of blood vessels and the Hb saturation index was evaluated using a prototype of PAM that has a flat scanning detector and is capable of simultaneously acquiring photoacoustic (PA) and ultrasound images. Next, another prototype of a PAM device with hemispherical sensors was developed to improve the visibility of the 3D structure of vessels by reducing the limited view effect. In clinical examination of breast cancer cases, the PAM system allowed 3D visualization of fine vessel networks with a spatial resolution of a half-millimeter and enabled us to determine the features of tumor-related vascular structures in human breast cancer. In addition, the oxygen saturation status of Hb was visualized using two different wavelengths, enabling more precise characterization of the tumor microenvironment. Results of clinical evaluation using our developed prototype of a PAM device confirmed that PA imaging technology has the potential to promote early detection of breast cancer, and realization of its practical use is expected in the near future.

Keywords Photoacoustic imaging · Mammography · Optoacoustic · Ultrasound · Vascularity · Oxygen saturation

1 Introduction

Japan's society is ageing more rapidly than ever before, and many other countries will face this issue in the near future. It is important to enable people to continue working by preserving their health and beauty in this super-aging society. Therefore, prevention and early detection of diseases and appropriate therapy are more important than ever. Such diseases as cancer, arteriosclerosis, rheumatism, and dementia are related to the disorder of vessels. Thus, the blood vessel networks and blood state must be monitored for early prediction of diseases and for health maintenance.

Clinics use different modalities of noninvasive vascular imaging, such as CT, MRI, and ultrasonic Doppler methods. However, CT and MRI angiography requires the use of a contrast medium and is limited by the high cost of testing; as a result, these techniques are unsuitable for mass screening and repeated examinations. The resolution of ultrasonic Doppler is not sufficient for imaging thinner vessels. In addition, the results of ultrasonography depend largely on instrument performance and the examiner's skill. Photoacoustic (PA) imaging offers better spatial resolution of ultrasound with high contrast optical absorption distribution for a deep area than purely optical imaging [1]. In addition, PA imaging provides the functional information state (e.g., blood oxygen saturation) in addition to the structure of vessels. PA imaging uses an ultrasound detector; as a result, it is suitable for multimodality diagnosis with ultrasound imaging [2].

Several reports have focused on optical imaging of the hemoglobin distribution and oxygenation state inside a tumor [3, 4]. They confirmed that angiogenesis is essential for breast cancer growth and is correlated with the

✉ Tsuyoshi Shiina
shiina.tsuyoshi.6w@kyoto-u.ac.jp

[1] Department of Human Health Sciences, Graduate School of Medicine, Kyoto University, 53 Kawahara-cho, Shogoin, Sakyo-ku, Kyoto 606-8507, Japan

[2] Department of Breast Surgery, Graduate School of Medicine, Kyoto University, 54 Kawahara-cho, Shogoin, Sakyo-ku, Kyoto 606-8507, Japan

[3] Japan Science and Technology Agency, ImPACT Program, Cabinet Office, K's Gobancho, 7, Gobancho, Chiyoda-ku, Tokyo 102-0076, Japan

malignant potential of a precursor lesion, and that hypoxia is associated with adverse effects on survival and response to treatment [5–7]. Therefore, clinical applications of PA imaging systems to the early diagnosis of cancer tumors are explored. We have investigated photoacoustic mammography (PAM) and developed different prototypes of PAM devices for clinical use in the Kyoto University/Canon joint research project (CK project) to acquire images for the diagnosis of breast cancer [8–12], and have demonstrated that 3D imaging can be realized with a resolution of a half-millimeter using the third prototype (PAM-03) [11, 12].

In addition to breast cancer diagnosis, the PA imaging device is also applied for detailed analyses of peripheral blood vessels, such as those in the palm. Matsumoto et al. reported on an analytical test of the blood vessel structure for exploratory clinical research, focusing on the twisting and winding of blood vessels to determine the shape of blood vessels in healthy subjects [13]. To expand the application of PA imaging to wider clinical fields such as 3D visualization technology for healthcare and non-medical purposes, we have been promoting a research and development program (the ImPACT program) with support from the cabinet office of Japan since 2014.

Here, we describe the developed prototypes of PAM systems and present some clinical results for the detection of human breast cancer.

2 Photoacoustic imaging technology

PA imaging is based on the photoacoustic effect as shown in Fig. 1. When an object is illuminated with light pulses from a laser, the absorber expands thermoelastically and the ultrasound waves, i.e., PA signals are emitted from the absorber. The PA signals are received simultaneously by multiple ultrasound sensors and used to form a 3D image of optical absorption [1]. PA imaging inherits advantages from both ultrasound imaging and optical imaging, such as safety, economy, ease of implementation, and high temporal and spatial resolution [2]. In addition, Photoacoustic imaging combines the high "optical contrast" with the deep penetration of "ultrasound imaging", making it possible to visualize clear images of locations deep inside the object. Matching the laser wavelength to the optical characteristics of the absorbers makes it possible to select each absorber (e.g., hemoglobin, melanin and lipid) to be visualized.

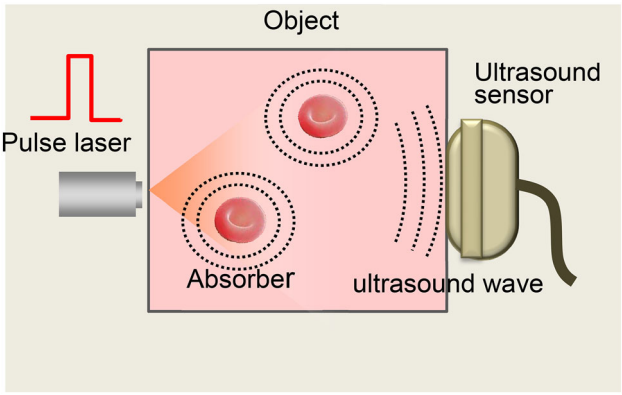

Fig. 1 Principle of photoacoustic imaging: when an object is illuminated with light pulses from a laser, the absorber expands thermoelastically and the ultrasound waves, i.e., PA signals are emitted from the absorber. The PA signals are received simultaneously by multiple ultrasound sensors and used to form a 3D image of optical absorption

PA imaging is able to produce high-resolution images of vascular structures such as tumor-related angiogenesis by matching the laser wavelength to hemoglobin [14]. In addition to morphological information, the PA imaging can provide functional information such as oxygen saturation of hemoglobin.

For example, if the absorption coefficient $\mu_a(\lambda_i)$ for different light wavelength λ_1 and λ_2 can correctly obtained, the hemoglobin (Hb) saturation value (SO_2) can be derived from the following equation [15]:

$$SO_2 = \frac{|HbO_2|}{|HbO_2| + |Hb|} = \frac{\frac{\mu_a(\lambda_2)}{\mu_a(\lambda_1)} \cdot \varepsilon_{Hb}(\lambda_1) - \varepsilon_{Hb}(\lambda_2)}{\varepsilon_{\Delta Hb}(\lambda_2) - \frac{\mu_a(\lambda_2)}{\mu_a(\lambda_1)} \cdot \varepsilon_{\Delta Hb}(\lambda_1)} \quad (1)$$

where ε_{Hb} is the molar extinction coefficient of deoxy-Hb and $\varepsilon_{\Delta Hb}$ is the difference in the molar extinction coefficients between deoxy-Hb and oxy-Hb (HbO_2). As above mentioned, angiogenesis and hypoxia are associated with the microenvironment of cancer, thus PA imaging has the potential to form the basis of diagnostic modalities for cancer.

3 Methods

3.1 3D photoacoustic mammography using a flat scanning detector

For breast cancer diagnosis, three prototypes of PAM were developed by our group in the CK project. The first and second PAM prototypes (PAM-01 and PAM-02) employed a flat scanning detector and a light delivery system from both the cranial and caudal directions. The major difference between PAM-01 and PAM-02 is the addition of US echo imaging. In PAM-02, a linear transducer array is used for US echo imaging. This paper outlines PAM-02, since its details such as specific parameters are reported in Ref. [10].

After setting the prone position in an appropriate direction (i.e., the craniocaudal (CC) or mediolateral

oblique (MLO) direction), one of the breasts is inserted into the opening and mildly compressed (50 N) between two transparent holding plates. A nanocomposite (NC) gel was adopted for acoustic coupling between the breast and the holding plate. Pulsed laser beams irradiate the breast from both sides (i.e., forward and backward) of the holding plates, and PA signals and ultrasound echo signals are detected on one side by each array transducer [10] (in Fig. 2).

A Ti:Sa laser pumped using a Q-switched Nd:YAG laser with a tunable wavelength of 700–900 nm was applied. Wavelengths of 756 and 797 nm were selected to construct a better image of the Hb saturation distribution after clinical evaluation of PAM visibility for different wavelengths (756, 797, 825, and 1064 nm). The light energy density of the backward laser was set to a maximum of 11 mJ/cm^2, and that of the forward laser was set to a maximum of 15 mJ/cm^2, which was higher than the backward laser to compensate the attenuation of PA signals from the deeper positions which were closer to the forward-side laser. These values were constant for both wavelengths and under the maximum permissible exposure (MPE) [26 mJ/cm^2 (756 nm) and 31 mJ/cm^2 (797 nm)].

As a detector of the PA signal, we employed a manufactured broadband capacitive micro-machined ultrasonic transducer (CMUT) [16] with 600 elements (20 × 30) and a central frequency of 2 MHz and fractional bandwidth of 130%. For US echo imaging, a linear transducer array with 6 MHz and 128 channels is dedicated because the CMUT device for the PA signal detector could not be applied to the US imaging frequency range of 6 MHz or more. The transducer of PA and US are scanned on the holding plate to measure a wide area of the breast. The subject's measurement area can be selected; for example, the measurement time is 7 min for scanning an area of 150 mm × 90 mm.

3.2 Reconstruction of absorption coefficient and Hb saturation index

The PA image was reconstructed using a modified universal back-projection (UBP) algorithm that corrects for acoustic refraction of the plate in front of the PA detector [17]. A phantom experiment indicated that PAM-02 can produce a PA image with a spatial resolution of 1 mm.

We used a PA image acquired at 795 nm to analyze the blood vessel structure (the image corresponding to the total hemoglobin distribution). Images of the Hb saturation value were derived from the acquisition of PA data using wavelengths of 756 and 797 nm [9, 10]. In practice, the accuracy of the calculated Hb saturation value (SO_2) has been questioned because of factors such as lack of system accuracy and fluence compensation. Therefore, as a relative value, we proposed the S-factor, (S_f), instead of SO_2, as follows [10]:

$$S_f = \frac{M \cdot \varepsilon_{\mathrm{Hb}}(\lambda_1) - \varepsilon_{\mathrm{Hb}}(\lambda_2)}{\varepsilon_{\Delta\mathrm{Hb}}(\lambda_2) - M \cdot \varepsilon_{\Delta\mathrm{Hb}}(\lambda_1)}, \quad M = \frac{\widetilde{\mu}_a(\lambda_2)}{\widetilde{\mu}_a(\lambda_1)} \tag{2}$$

where $\widetilde{\mu}_a(\lambda)$ is the apparent light absorption coefficient at wavelength λ of the absorber measured by PA imaging system and M is the relative parameter of the measured absorption coefficient of λ_2 divided by that of λ_1. The reliability of M is considered to be affected by the accuracy of the estimation of light fluence for each wavelength, which may be related to the depth and/or complexity of the

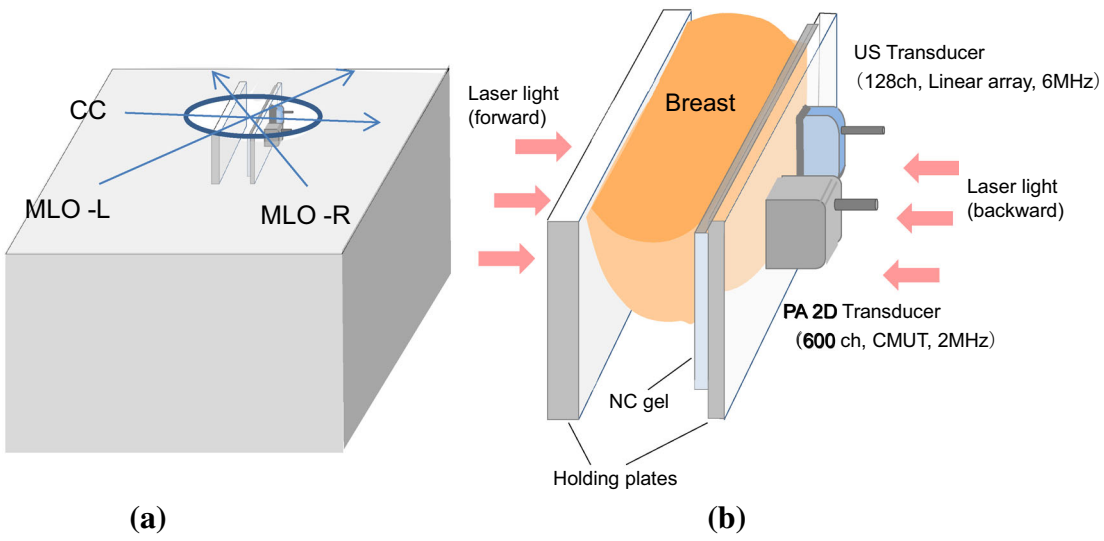

Fig. 2 Schematic illustration of **a** axes of the body for measurement in the CC and MLO positions, **b** schematic illustration of the structure of the holding plates of PAM-02

tissues. S_f is also expected to provide meaningful information in vivo.

3.3 Development PAM with a hemispherical array detector

In the next stage, the third prototype of PAM with hemispherical sensors (PAM-03) was developed by the CK project in collaboration with Optosonics, Inc. (USA) to reduce the effect of limited view and improve the visibility of the 3D structure of vessels, and its clinical evaluation was conducted [11, 12, 19].

Figure 3a depicts the PAM-03 system. The patient lies prone on a bed and places one breast in a hemispherical breast holding cup, which is filled with body-temperature water. The hemispherical detector array is located under the holding cup (Fig. 3b). This detector has 512 elements, each 3 mm in diameter and with a 2 MHz of central frequency on the inside surface (Fig. 3c).

The detector array was scanned continuously in a spiral pattern within a plane in an effort to improve image quality at the center of the breast cup, which corresponded to the deep tissue. In the PAM-03 system, a Q-switched alexandrite laser with selectable wavelengths of 755 and 795 nm was used to evaluate the Hb saturation index of the blood vessels. The diameter of light illumination was 60 mm at the surface of the breast cup. The maximum light energy was set to less than 10 mJ/cm^2.

The range of the cylinder's 30 mm radius is measured using one laser shot. The total imaging area can be increased by scanning the detector in the horizontal plane up to 100 mm radius. Data acquisition time depends on the number of measurement points. For example, it takes 102.4 s for 2048 points at one scan. With measurement using two wavelengths for calculating the Hb saturation index, double the measuring time (4 min) for data acquisition at 2048 points is required.

According to the evaluation of spatial resolution using a spherical phantom, full width at half maximum along the

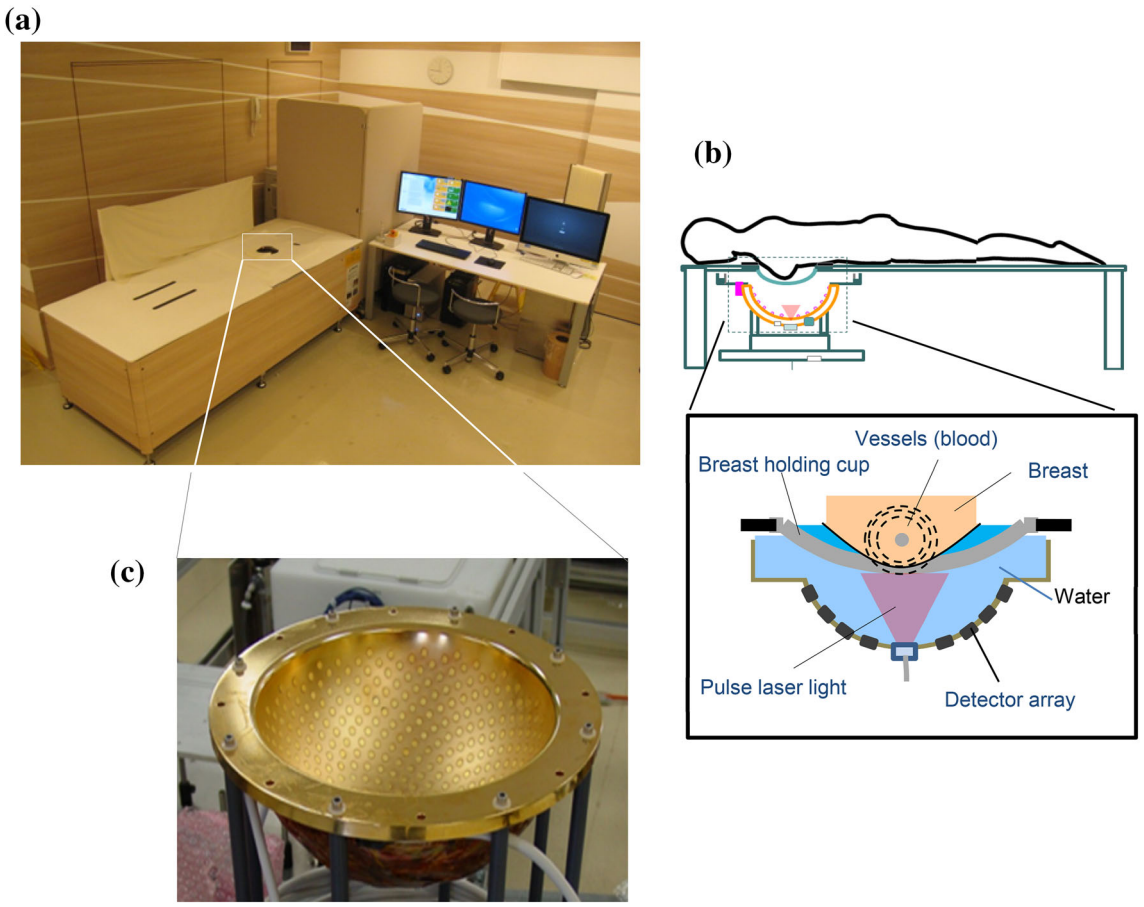

Fig. 3 Photoacoustic mammography with hemispherical sensors (PAM-03). **a** PAM-03 system. **b** The patient lies prone on the bed and places one breast in a hemispherically shaped breast holding cup, which is filled with body-temperature water. The hemispherical detector under the holding cup was scanned continuously in a spiral pattern within a plane at the center of the breast cup. **c** Hemispherical detector array with 512 elements and 2 MHz central frequency

horizontal direction was 0.57 mm, and that along the vertical direction was 0.37 mm.

3.4 Compensation of sound speed deviation and body motion

PA image reconstruction in PAM-03 also employs a UBP algorithm, which needs speed distribution within the measurement area [18]. Therefore, the discrepancy between true speed distribution and given values greatly affects the performance of image reconstruction. In an effort to reduce degradation of the image resolution, both the average sound speed of the patients' breast and that of water were considered for PA image reconstruction. The light absorption coefficient (μ_a) and Hb saturation index (S-factor) were calculated similarly to PAM-02. With PAM-03, the breast in the holding cup is easier to move during the scanning process than with PAM-02. Reconstruction of the μ_a and S-factor images is extremely susceptible to body motion because PA signals measured using multiple laser shots at different portions and wavelengths are integrated to calculate the μ_a and S-factor. The first step of body motion correction is estimation of movement vectors of body motion by calculating the correlation between images obtained by multiple laser shots. PA images for each wavelength are obtained by integration of images by multiple shots, which are corrected by movement vectors. The second step of motion correction is conducted between PA images for two different wavelengths using free-form deformation [19] to deform the breast shape of the 755 nm image toward that of the 795 nm image.

4 Results and discussion

4.1 Analysis of a Tumor-related vascular structure using the PAM-02 system

The ability of a PAM system to detect breast cancer lesions was demonstrated. Figure 4 presents PA images of the subcutaneous blood vessel of a breast obtained using PAM-02 with a wavelength of 797 nm. Figure 4 presents three images of the cross-sections orthogonal to each other. Figure 4a is a maximum intensity projection (MIP) image at a depth of 8–9.75 mm from the front view of the holding plate (C-mode) and clearly visualizes the network of subcutaneous blood vessels in a wide area. Figures 4b, c are images from the side views (B-mode) in the elevational and lateral directions, and the connectivity of vessels is not as clear as in Fig. 4a. One main reason is that the limited view of the plane PA transducer affects the imaging of vessels in the depth direction.

Figure 5 presents (a) an S-factor distribution image (MIP image at a depth of 15–19 mm) of the lesion of invasive ductal carcinoma (IDC) and (b) an S-factor image overlaid on a US image (slice image at a depth of 15 mm) obtained using the PAM-02 system. Many blood vessel-like signals were observed around the tumor in the US low-echo image. Furthermore, it can be determined that the signals run centripetally toward the center of the tumor, and that signal intensities become disrupted or weakened at the border of the tumor. Thus, we were able to analyze the angioarchitecture of tumor-related blood vessels [10].

4.2 Clinical study of breast cancer diagnosis using the PAM-03 system

Speed distribution estimation and body motion correction were validated using PA signals of a volunteer's palm obtained by PAM-03. Figure 6a presents a PA image of a palm reconstructed at a voxel size of 0.125 mm using a given speed of tissue and without correction of body motion. Vessel images, especially the upper part, are blurred; and the structure of thin vessels is difficult to recognize. A PA image after adaptively estimating speed and correcting for body motion is presented in Fig. 6b. Figure 6c depicts the estimated movement vector of body motion during a spiral scan of the detector. Visibility of the vessel structure is clearly improved in Fig. 6b.

Figure 7a presents an MIP image of the whole breast with an invasive breast carcinoma obtained using PAM-03 [12]. After eliminating PA signals from subcutaneous vessels at a depth of 4 mm, an MIP image around the tumor area was displayed (Fig. 7b). Figure 7c is a fusion image of PA and MRI magnified around the tumor. The MR image was deformed by overlaying the major corresponding blood vessels between MRI and PA images. The fusion image of PA and MRI is useful for precisely visualizing the tumor location on PA images. Including the case depicted in Fig. 7, clinical evaluation of PA images for many cases of breast cancer allowed detecting centripetal blood vessels and vessel disruption or rapid narrowing at the boundary of the tumor as a feature of tumor-related vessels [12].

4.3 Challenges for clinical translation of PA imaging

As outlined above, our developed prototypes of PAM demonstrated that the 3D-PA image of vessel structure in a deeper zone of the breast can be achieved with a spatial resolution of 0.57 mm. With the present system, the imaging region is limited to about 30 mm depth. Measurement time for a scan with two wavelengths takes 4 min. Consequently, the body motion of patients often

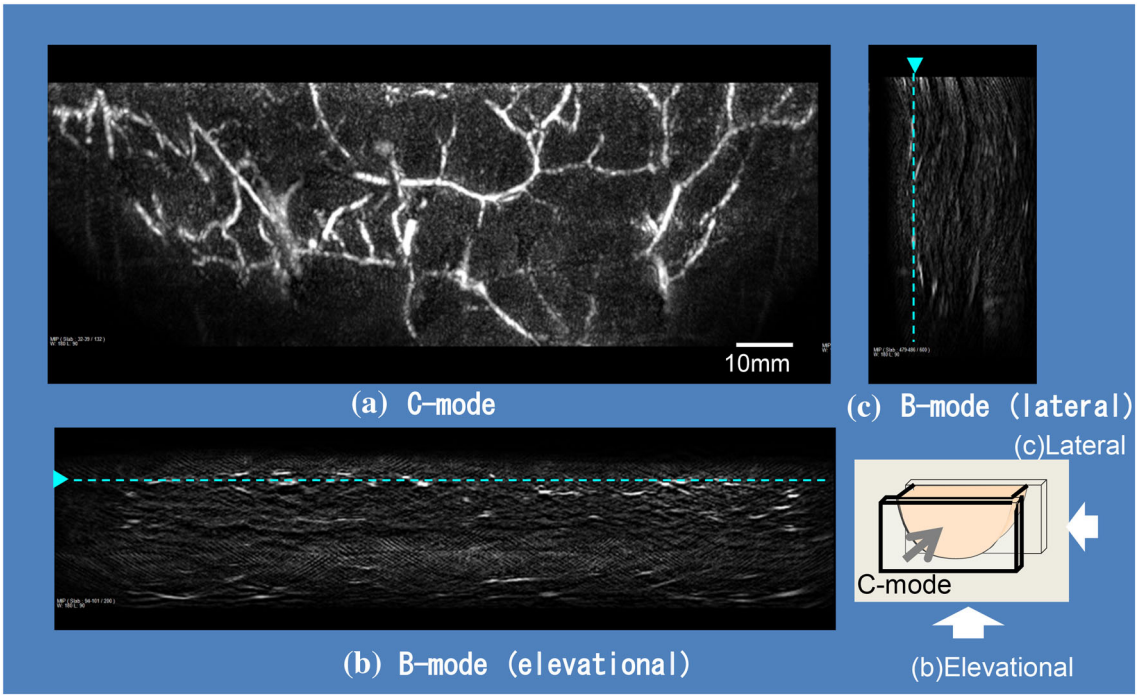

Fig. 4 PA images of the subcutaneous blood vessel of a breast obtained using PAM-02 (MLO-L) with a wavelength of 797 nm. **a** MIP image at a depth of 8.0–9.75 mm from the front view of the holding plate (C-mode) to visualize the network of subcutaneous blood vessels in a wide area. **b**, **c** Images from the side view (B-mode) in the elevational direction and lateral direction. The dashed limes in (**b**) and (**c**) correspond to the cross-section position of the C-mode figure

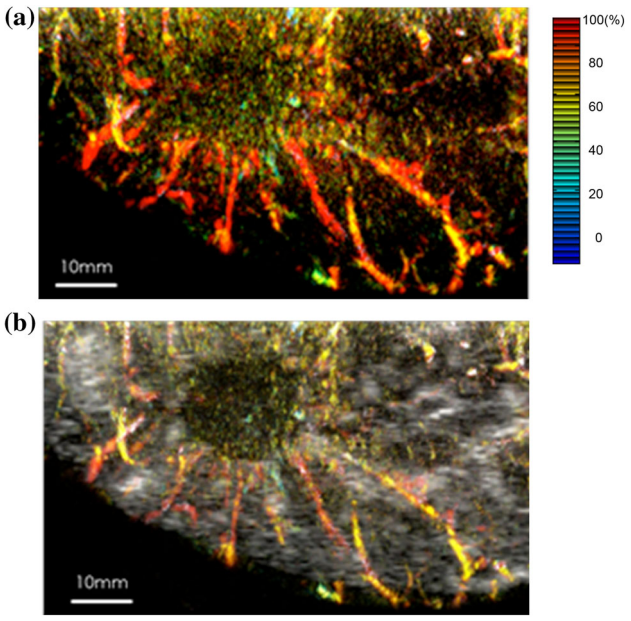

Fig. 5 S-factor and US images of the lesion of IDC obtained using the PAM-02 system. **a** S-factor distribution image, displayed by color scale from blue to red as S-factor increases from 0 to 100%. **b** Fusion image of S-factor and US C-mode image. Many blood vessel-like signals were observed around the tumor in the US low-echo image. Furthermore, it was determined that the signals run centripetally toward the center of the tumor, and signal intensities become disrupted or weakened at the border of the tumor. (Color figure online)

degrades image quality and S-factor accuracy even with the use of the body motion compensation. Therefore, further technological advances should be incorporated to speed up data acquisition and processing, and to improve three-dimensional resolution at deep tissue levels.

To address these challenges and promote the clinical translation of PA imaging technology, the development of PAM is passed from the CK project to the Impulsing Paradigm Change through Disruptive Technology (ImPACT) program entitled "Innovative visualization technology to create a new growth industry", which started with support from the cabinet office of Japan in 2014 [20]. The objective of the program is to develop new 3D visualization technology based on PA imaging that can image the state of the human body noninvasively and material objects nondestructively, to enable early diagnosis of diseases and inspection of industrial materials in an effort to increase safety and security. This program is conducted through several projects covering (1) base technologies for visualization using PA technology, (2) tunable lasers adapted to the absorption spectrum of the human body and substances, (3) ultrasound sensor arrays with high bandwidth and high sensitivity, (4) visualization system development, and (5) evaluation of the applicability in the medical and quality examination fields.

Biomedical imaging is still the main objective of the ImPACT program. Plans include developing a 3D real-time

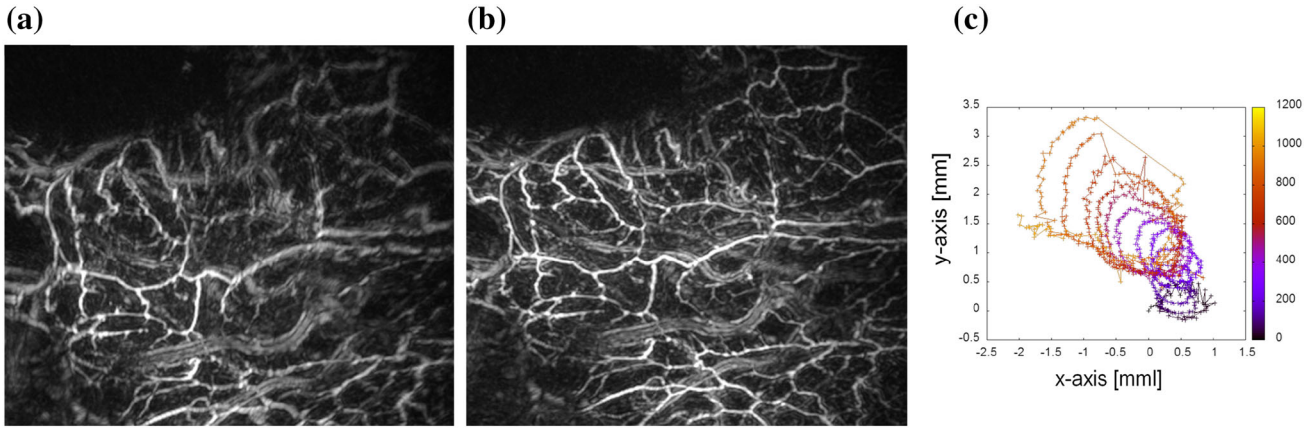

Fig. 6 Image quality improvement by speed distribution estimation and body motion correction during a spiral scan of the detector **a** without processing and **b** with processing. **c** Estimated movement vector of body motion during a spiral scan of the detector. Images of vessels in (**a**) are blurred and the structure of thin vessels is difficult to determine, while visibility of the vessel structure is clearly improved in (**b**)

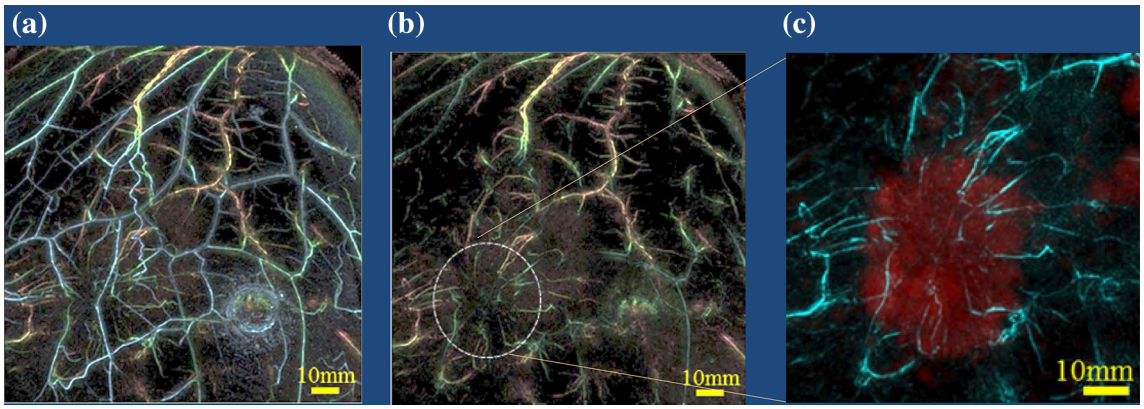

Fig. 7 Clinical evaluation of breast cancer imaging by PAM-03. **a** MIP image of the whole breast for an invasive breast carcinoma obtained using PAM-03. **b** MIP image around the tumor area after eliminating PA signals from subcutaneous vessels at a depth of 4 mm. **c** Fusion image of PA (cyan) and MRI (red) magnified around the tumor. Centripetal blood vessels and vessel disruption at the boundary of the tumor could be observed as a feature of tumor-related vessels [12]. (Color figure online)

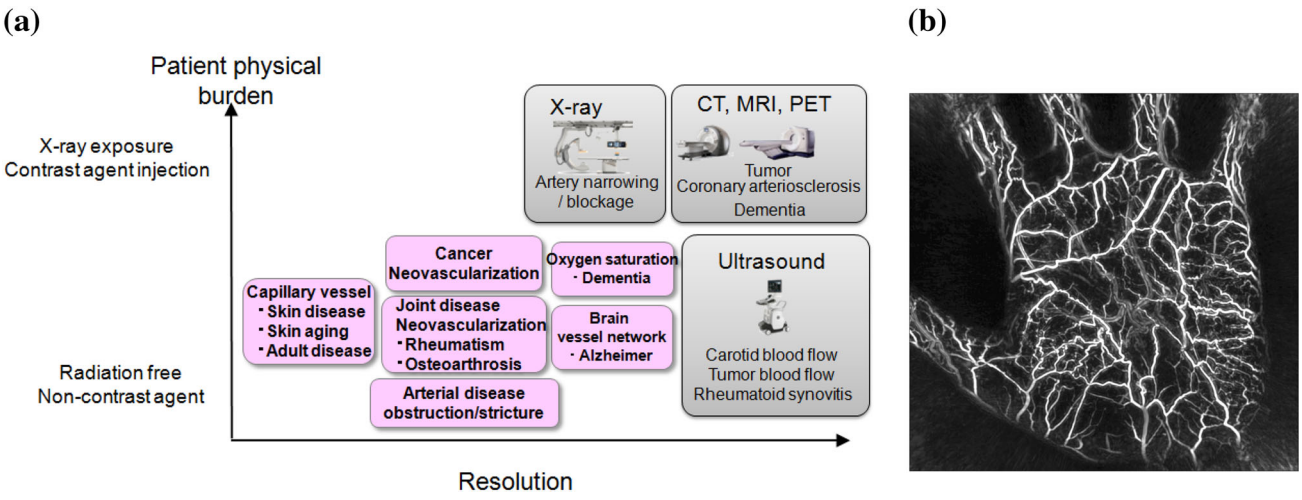

Fig. 8 ImPACT program for promoting Vascular Health Sciences [17]. **a** Examples of using PA technologies in medicine and healthcare. **b** PA image of a human palm obtained using the PAM-03 system

PA imaging system (Fig. 8). It will be applicable for wider clinical fields (e.g., cancer diagnosis, orthopedics, dermatology, plastic surgery, and dementia), as well as health and beauty care. In addition, we aim to foster Vascular Health Science, a new health science field, to contribute to early prediction of diseases and health maintenance by monitoring blood vessel networks and blood state in the human body to enable people to continue working while preserving their health and beauty in the super-aging society [21].

5 Conclusion

We developed PAM prototypes and demonstrated that 3D-PA images of vessel networks in the breast with a spatial resolution of 0.57 mm were obtained using a PAM system with a hemispherical detector array. In clinical examination of breast cancer cases, the PAM system enabled visualizing fine vasculature that is not visible on standard contrast-enhanced MRI and determining the features of tumor-related vascular structures in human breast cancer. In addition, the oxygen saturation status of Hb was visualized using two different wavelengths, enabling more precise noninvasive characterization of the tumor microenvironment.

In addition to these primary merits of PA imaging, the PA imaging system is expected to combine ultrasound imaging that provides detailed morphological information in real time. The US and PA fusion image created using the PAM-02 system enabled us to overlay a tumor-related vasculature image onto tumor mass images. Although PAM-03 was dedicated for PA imaging for simplification, a system combined with US and PA imaging should be investigated in future work.

As is true with other medical imaging technologies, some challenges remain in achieving clinical applications of a PA imaging system. Such challenges include simultaneous pursuit of high-resolution and high-speed imaging [22], sufficient imaging quality in deep tissue, and quantification for high-quality functional imaging such as blood oxygen saturation [23]. In addition, for practical use of the PAM system in clinics, developing a downsized, low-cost laser device is also important. We believe that in the near future these challenges will be overcome and PA imaging will become a powerful modality in medicine.

Acknowledgements The authors thank all members of the CK project at Kyoto University Hospital and Canon, Inc., for collaboration of PAM research and analyzing clinical data.

Funding This study was funded by the CK project "Innovative Techno-hub for Integrated Medical Bio-imaging" supported by the Ministry of Education, Culture, Sports, Science, and Technology, Japan, and the ImPACT Program "Innovative visualization technology to create a new growth industry" supported by the Council for Science, Technology and Innovation, Cabinet Office, Japan.

Compliance with ethical standards

Conflict of interest Takayuki Yagi is an employee of Canon Inc., Japan and temporarily transferred to the Japan Science and Technology Agency. Canon Inc. designed and invented the photoacoustic mammography system used in this study. The other authors have no conflict of interest.

Ethical approval The present study was approved by the Ethics Committee of the Kyoto University Graduate School of Medicine. This study was conducted in accordance with the Declaration of Helsinki.

Informed consent Written informed consent was obtained from all participants included in the study.

References

1. Kim C, Favazza C, Wang LV. In vivo photoacoustic tomography of chemicals: high-resolution functional and molecular optical imaging at new depths. Chem Rev. 2010;110:2756–82.
2. Kim J, et al. Programmable real-time clinical photoacoustic and ultrasound imaging system. Sci Rep. 2016;6:35137.
3. Pogue BW, et al. Implicit and explicit prior information in near-infrared spectral imaging: accuracy, quantification and diagnostic value. Philos Trans R Soc A. 2011;369:4531–57.
4. Quarto G, et al. Estimate of tissue composition in malignant and benign breast lesions by time-domain optical mammography. Biomed Opt Express. 2014;5:3684–8.
5. Viacava P, et al. Angiogenesis and VEGF expression in pre-invasive lesions of the human breast. J Pathol. 2004;204:140–6.
6. Makris A, et al. Reduction in angiogenesis after neoadjuvant chemoendocrine therapy in patients with operable breast carcinoma. Cancer. 1999;85:1996–2000.
7. Milani M, Harris AL. Targeting tumour hypoxia in breast cancer. Eur J Cancer. 2008;44:2766–73.
8. Kitai T, et al. Photoacoustic mammography: initial clinical results. Breast Cancer. 2014;21(2):146–53.
9. Fakhrejahani E, et al. Clinical report on the first prototype of a photoacoustic tomography system with dual illumination for breast cancer imaging. PLoS ONE. 2015;10:e0142287.
10. Asao Y, et al. Photoacoustic mammography capable of simultaneously acquiring photoacoustic and ultrasound images. J Biomed Opt. 2016;21(11):116009.
11. Kruger RA, et al. Dedicated 3D photoacoustic breast imaging. Med Phys. 2013;40:113301.
12. Toi M, et al. Visualization of tumor-related blood vessels in human breast by photoacoustic imaging system with a hemispherical detector array. Sci Rep. 2017;7:41970.
13. Matsumoto Y, et al. Label-free photoacoustic imaging of human palmar vessels: a structural morphological analysis. Sci Rep. 2018;8:786.
14. Zhang HF, et al. Functional photoacoustic microscopy for high-resolution and noninvasive in vivo imaging. Nat Biotechnol. 2006;24(7):848.
15. Wang X, et al. Noninvasive imaging of hemoglobin concentration and oxygenation in the rat brain using high-resolution photoacoustic tomography. J Biomed Opt. 2006;11(2):024015.

16. Wygant O, et al. Integration of 2D CMUT arrays with front-end electronics for volumetric ultrasound imaging. IEEE Trans Ultrason Ferroelectr Freq Control. 2008;55:327–42.
17. Fukutani K, et al. Characterization of photoacoustic tomography system with dual illumination. Proc SPIE. 2011;7899:78992J.
18. Xu M, Wang LV. Universal back-projection algorithm for photoacoustic computed tomography. Phys Rev E. 2005. https://doi.org/10.1103/physreve.71.016706.
19. Sederberg TW. Free-form deformation of solid geometric models. Proc SIGGRAPH'86. 1986;20(4):151–60.
20. Home page of the ImPACT program, Cabinet Office in Japan; http://www.jst.go.jp/impact/program/10.htm.
21. Shiina T. Innovative photoacoustic imaging technology to support vascular health science. In: Proceedings of CLEO 2016, ATh4N.3; 2016.
22. Meng J, Wang LV, Ying L, Liang D, Song L. Compressed-sensing photoacoustic computed tomography in vivo with partially known support. Opt Express. 2012;20(15):16510–23.
23. Xia J, Danielli A, Liu Y, Wang L, Maslov K, Wang LV. Calibration-free quantification of absolute oxygen saturation based on the dynamics of photoacoustic signals. Opt Lett. 2013;38(15):2800–3.